Diastereo-Differentiating Hydride Transfer at Bridged NAD(H) Models[1]

Frank Rob, Hendrik J. van Ramesdonk, Willem van Gerresheim, Peter Bosma, Jacques J. Scheele, and Jan W. Verhoeven*

Contribution from the Laboratory for Organic Chemistry, University of Amsterdam, Nieuwe Achtergracht 129, 1018 WS Amsterdam, The Netherlands. *Received October 3, 1983*

Abstract: Five NAD(H) models are described which contain the 1-benzyl(dihydro)pyridine-3,5-diamide moiety as a redox center. This redox center is bridged by various $CH_2CH_2ArCH_2CH_2$ groups connecting the amido nitrogens and thereby incorporating the redox center into a cyclophane framework. X-ray structure data as well as ^1H NMR studies reveal a profound influence of the nature of the aryl group (Ar) on the molecular and magnetic symmetry of the environment in which the redox center resides. In three of the cyclophanes this leads to a distinct anisochronism of the C(4) hydrogens at the reduced redox center (i.e., the 1,4-dihydropyridine moiety), analogous to the anisochronism observed for the C(4) hydrogens in **NAD(P)H**. Deuterium isotope exchange studies show that the diastereotopism of the C(4) positions revealed by the NMR data also leads to a distinct diastereo-differentiation in hydride (deuteride) exchange processes at C(4). These systems thereby constitute the first examples of NAD(H) models capable to mimic the diastereo-differentiating course of hydride exchange at pyridine dinucleotides under enzymatic conditions. The degree of diastereo-differentiation amounts to 67% for Ar = 1,4-naphthylene and to more than 90% for two cyclophanes in which the Ar group is a substituted 1,3-phenylene moiety. From X-ray structure data and from electronic absorption spectra it is concluded that in all reduced cyclophanes the strain exerted by the bridge leads to a boat-shape distortion of the 1,4-dihydropyridine moiety, which places the C(4) hydrogens in axial and equatorial orientations. Interestingly the distortion of the dihydropyridine moiety was found to be most pronounced in the two cyclophanes displaying the highest degree of diastereo-differentiation. Furthermore it could be shown that in all cases hydride exchange preferentially occurs via the axial C(4) position. Kinetic investigation of the hydride-exchange processes suggests that a (partial) boat shape of the pyridine ring also occurs in the transition state. It is therefore concluded that diastereo-differentiating hydride exchange at the cyclophanes may largely be attributed to stereoelectronic effects which favor exchange at an axial site. Since comparison of free and enzyme-bound NAD(P)H fails to reveal a distortion of the dihydronicotinamide chromophore in the latter, such distortion is concluded to be of minor importance in the enzymatic diastereo-differentiation. A model based on "positive-differentiation" is proposed, which links enzymatic diastereo-differentiation to enzymatic catalysis and in which selective catalysis of hydride transfer at one of the diastereotopic C(4) positions leads to a diastereo-differentiation which equals the catalytic effect of the enzyme. This model is in agreement with recent findings concerning the orientation of the nicotinamide ring in enzyme-bound NAD(P)H.

1. Introduction

In the coenzymes NADH and NADPH the two reactive hydrogens at C(4) of the nicotinamide moiety occupy diastereotopic positions. This leads to a chemical shift difference readily detectable[2,3] by ^1H NMR spectroscopy but only to a minor—if any[2]—difference in chemical reactivity in the free coenzymes. The latter situation changes dramatically upon complexation of these coenzymes with enzymes of the dehydrogenase family. Such holoenzymes in general[4-6] mediate hydride-transfer processes with an extremely high degree of diastereo-differentiation.[7] Several factors have been proposed to explain this high degree of diastereo-differentiation in the enzymatic process. As early as 1957 Levy and Vennesland[8] suggested the rather flexible dihydronicotinamide ring of NAD(P)H to adopt a specific (pseudo)boat shape at the enzyme surface, which leads to (pseudo)axial and (pseudo)equatorial orientations of the C(4) hydrogens. Recently Buck et al.[9,10] tentatively proposed yet another specific distortion of the dihydronicotinamide chromophore, involving rotation of the amide group with respect to the pyridine ring, to be linked to the induction of diastereo-differentiation.

Table I. ^1H Chemical Shift (at 20 °C[a] in $CDCl_3$ Relative to Me_4Si) and Geminal Coupling of C(4) Protons in $\mathbf{1H_2}$–$\mathbf{6H_2}$[b]

compd	$\delta_{C(4)H_2}$ H_A	H_B	$^2J_{AB}$, Hz
$\mathbf{1H_2}$	1.95		
$\mathbf{2H_2}$	2.08		
$\mathbf{3H_2}$	2.12	1.43	(−) 13
$\mathbf{4H_2}$	2.61	2.48	(−) 14
$\mathbf{5H_2}$	2.56	2.48	(−) 14
$\mathbf{6H_2}$	3.26		
β-NADH	2.73[c]	2.64[c]	(−) 18 ± 1

[a] Chemical shifts of the cyclophanes are essentially unchanged by temperature variation (range studied, −30 to +40 °C). [b] Corresponding data [3,6] for β-NADH (22 °C, aqueous buffer relative to DSS) have been added for comparison. [c] Chemical shifts depend strongly upon temperature; the AB pattern collapses to a singlet above 74 °C in a 220-MHz spectrum.[2,3,6]

An interesting correlation between enzymatic diastereo-differentiation and the syn or anti orientation of the nicotinamide group in the enzyme-bound coenzyme was recently proposed by Benner et al.[11,12] This orientation is thought to determine not only the selective accessibility of one of the diastereotopic faces

(1) For a preliminary communication, see: Rob, F.; Verhoeven, J. W.; van Ramesdonk, H. J.; Pandit, U. K.; de Boer, Th. J. *Tetrahedron Lett.* **1980**, *21*, 1549-1552.
(2) Sarma, R. H.; Kaplan, N. O. *Biochemistry* **1970**, *9*, 539-548.
(3) Oppenheimer, N. J.; Arnold, L. J.; Kaplan, N. O. *Proc. Natl. Acad. Sci. U.S.A.* **1971**, *68*, 3200-3205.
(4) Fisher, H. F.; Conn, E. E.; Vennesland, B.; Westheimer, F. H. *J. Biol. Chem.* **1953**, *202*, 687-697.
(5) Bentley, R. "Molecular Asymmetry in Biology"; Academic Press: New York, 1961; Vol. II, Chapter 1.
(6) Oppenheimer, N. J.; Kaplan, N. O. *Bioorg. Chem.* **1974**, *3*, 141-153.
(7) The lucid and complete stereochemical nomenclature of Izumi and Tai is adopted; see: Izumi, Y.; Tai, A. "Stereo-differentiating Reactions"; Academic Press: New York, 1977.
(8) Levy, H. R.; Vennesland, B. *J. Biol. Chem.* **1957**, *228* 85-96.
(9) Donkersloot, M. C. A.; Buck, H. M. *J. Am. Chem. Soc.* **1981**, *103*, 6554-6558.
(10) Brounts, R. H. A. M.; Buck, H. M. *J. Am. Chem. Soc.* **1983**, *105*, 1284-1288.
(11) Benner, S. A. *Experientia* **1982**, *38*, 633-637.
(12) Nambiar, K. P.; Stauffer, D. M.; Kolodziej, P. A.; Benner, S. A. *J. Am. Chem. Soc.* **1983**, *105*, 5886-5890.

0002-7863/84/1506-3826$01.50/0

Chart I. Structure and Abbreviated Notation of Cyclophanes (Top) and Other Relevant Compounds Used in This Study

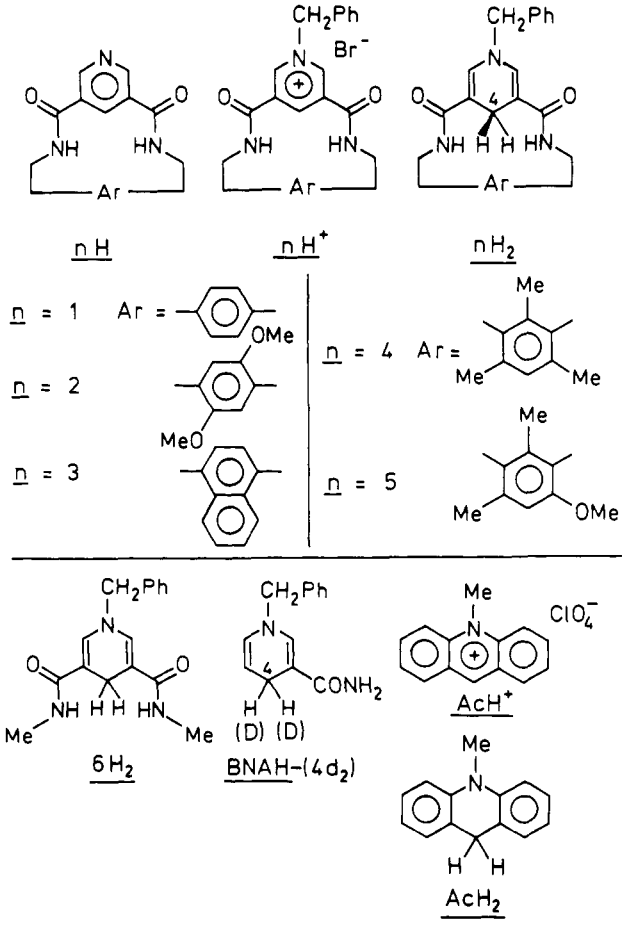

of the nicotinamide ring but also to influence the reducing power of the coenzyme thereby enabling the enzymatic system to achieve optimal catalytic activity for a particular substrate.[11-13] In a preliminary communication[1] we suggested that differential accessibility of the nicotinamide faces might be mimicked in bridged coenzyme models in which the bridge specifically inhibits substrate access at one face of the pyridine ring. A single example of such a bridged model ($\mathbf{4H^+}$) was furthermore provided and shown[1] to incorporate deuterium with a high degree of diastereo-differentiation upon reduction ($\mathbf{4H^+} \rightarrow \mathbf{4HD}$) with a deuteride donor.

The present paper reports the synthesis of $\mathbf{4H^+}$ as well as a number of related bridged coenzyme models and describes a study of the diastereo-differentiation observed upon hydride addition and abstraction as well as of the kinetics of these processes. Chart I summarizes the structure and numbering or abbreviated notation of the compounds and relevant reagents mentioned in this study.

2. Results and Discussion

(2.1) ^{1}H NMR Detection of Diastereotopic C(4) Protons in $\mathbf{nH_2}$. In order to enable direct detection by ^{1}H NMR spectroscopy of diastereoface-differentiation during the transformation $\mathbf{nH^+} \rightarrow \mathbf{nH_2}$ the eventual diastereotopism of the C(4) protons in the latter must lead to a detectable anisochronism. The presence of the magnetically anisotropic Ar group in the bridged compounds ($\mathbf{1H_2}$–$\mathbf{5H_2}$) is expected to warrant such anisochronism if the spatial disposition of the C(4) hydrogens toward this Ar group is different. As evident (cf. Table I) from a comparison of the chemical shift data of the bridged compounds ($\mathbf{1H_2}$–$\mathbf{5H_2}$) with those of the nonbridged model $\mathbf{6H_2}$ the Ar group exerts a strong shielding effect on both C(4) protons. In $\mathbf{1H_2}$ and $\mathbf{2H_2}$, however, these protons retain the isochronism characteristic for "normal" nonbridged

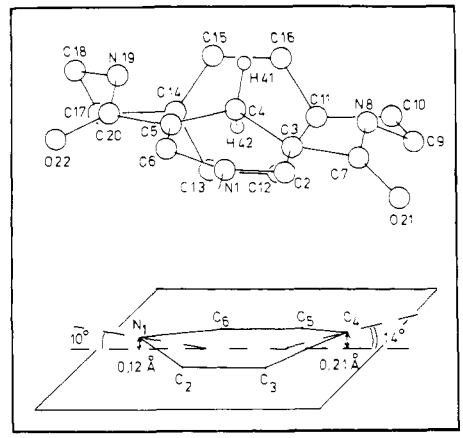

Figure 1. X-ray structure[14] of $\mathbf{1H_2}$, the benzyl substituent has been omitted for clarity. The geometry of the dihydropyridine ring is defined at the bottom.

Table II. Electronic Absorption Data for the Long-Wavelength Transition of the Dihydropyridine Chromophore in Cyclophanes $\mathbf{1H_2}$–$\mathbf{5H_2}$ as well as in the Nonbridged Model Compound $\mathbf{6H_2}$

compd	solvent	λ_{max}, nm	ϵ_{max}, L mol^{-1} cm^{-1}
$\mathbf{6H_2}$	dimethyl sulfoxide	376	6600
	water	382	7600
$\mathbf{1H_2}$	water	372	5000
$\mathbf{2H_2}$	water	372	4600
$\mathbf{3H_2}$	methanol	372	4600
$\mathbf{4H_2}$	methanol	344	3600
$\mathbf{5H_2}$	methanol	348	3800

1,4-dihydropyridines such as $\mathbf{6H_2}$. On the basis of X-ray data (vide infra) it seems plausible that in the time-averaged conformation of $\mathbf{1H_2}$ and $\mathbf{2H_2}$ in solution the Ar ring and the dihydropyridine ring are effectively perpendicular with the N(1)–C(4) axis of the pyridine ring pointing toward the center of Ar. This leads to effective C_{2v} symmetry for $\mathbf{1H_2}$ (i.e., homotopic C(4) protons) and C_2 symmetry for $\mathbf{2H_2}$ (i.e., enantiotopic C(4) protons).

While the effective isochronism of the C(4) protons in $\mathbf{1H_2}$ and $\mathbf{2H_2}$ is maintained even at low temperature (−40 °C), the C(4) protons of the other cyclophanes are anisochronous (cf. Table I) at all temperatures studied (−30 to +40 °C). The chemical shift difference for $\mathbf{4H_2}$ and $\mathbf{5H_2}$ is nearly equal (~0.1 ppm) and comparable to that reported[2,3,6] for the diastereotopic C(4) protons in β-NADH while a much larger chemical shift difference is observed for $\mathbf{3H_2}$ (0.69 ppm). Interestingly the geminal coupling constant in the cyclophanes (13–14 Hz) is significantly smaller than that reported[2] (~18 Hz) for NADH. This probably has to be attributed to the presence of the extra electron-withdrawing amide group at C(5) in the cyclophanes.

(2.2) Nonplanarity of the Dihydropyridine Chromophore in the Cyclophanes. For $\mathbf{1H_2}$ crystals suitable for X-ray structure determination could be grown. The results of this analysis have been published[14] in full, and Figure 1 depicts the conformation found. The Ar and dihydropyridine ring make a large angle (~70°). As discussed above time-averaged perpendicularity of these rings seems to occur in solution, possibly via rapid interconversion between the conformation depicted in Figure 1 and its mirror image.

Both amide groups adopt a nearly planar syn conformation and are almost coplanar (twist angles ≤ 20°) with the C(2)–C(3) and C(5)–C(6) double bonds, which allows their N–H protons to fit between the C(4) protons. In this respect the dihydropyridine chromophore of $\mathbf{1H_2}$ strongly resembles that of the nonbridged system $\mathbf{6H_2}$ for which X-ray diffraction studies[15] revealed a similar

(13) For a recent discussion of factors determining optimal catalytic activity, see: Chin, J. *J. Am. Chem. Soc.* **1983**, *105*, 6502–6503.

(14) van Herk, A. M.; Goubitz, K.; Overbeek, A. R.; Stam, C. H. *Acta Crystallogr., Sect. B* **1982**, *B38*, 490–494.

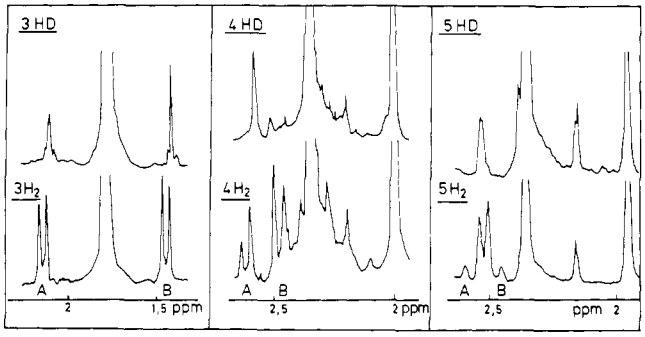

Figure 2. Partial ^{1}H NMR spectra (360 MHz for **n** = **3** and **4**, 250 MHz for **n** = **5**) of $\mathbf{nH_2}$ and **nHD** in $CDCl_3$ at room temperature.

amide orientation, which is also observed[16] for **BNAH** in the solid state. Whereas, however, the dihydropyridine ring of **BNAH** and of $\mathbf{6H_2}$ is planar, that of $\mathbf{1H_2}$ is found[14] to adopt a pseudoboat conformation with N(1) and C(4) deviating 0.12 and 0.21 Å, respectively, from the plane defined by C(2), C(3), C(5), and C(6) (see Figure 1). Apparently this distortion of the rather flexible[17,18] dihydropyridine ring alleviates part of the strain in the macrocyclic cyclophane system. This phenomenon has been observed before in bridged[19] and otherwise sterically congested dihydropyridines.[20]

Hypso- and hypochromic effects in the electronic absorption spectrum of $\mathbf{1H_2}$ as compared to $\mathbf{6H_2}$ (see Table II) indicate that a significant distortion of the dihydropyridine chromophore of the former is retained in solution.

The UV data for cyclophanes $\mathbf{2H_2}$ and $\mathbf{3H_2}$ indicate a chromophore distortion comparable to that in $\mathbf{1H_2}$. In cyclophanes $\mathbf{4H_2}$ and $\mathbf{5H_2}$, which contain a 1,3-connected Ar group instead of a 1,4-connected Ar group, the distortion appears to be more severe leading to a large hypsochromic shift and hypochromic effect (~50%) for the long-wavelength dihydropyridine transition. Clearly the effective shortening of the bridge by substituting a 1,3-connected Ar group for a 1,4-connected Ar group significantly enhances the strain exerted on the dihydropyridine chromophore.

The possible effect of the distortion of the dihydropyridine group on the diastereodifferentiating reactivity of the C(4) hydrogens is discussed in the next sections.

(2.3) Diastereoface-Differentiation[7] in the Reaction $\mathbf{nH^+}$ → nHD. As evident from the ^{1}H NMR data presented above reduction of the cyclophanes $\mathbf{3H^+}$–$\mathbf{5H^+}$ with a deuteride donor may lead to the diastereomers[21] $\mathbf{nH_AD_B}$ and $\mathbf{nH_BD_A}$ that can be discerned by NMR spectroscopy.

BNAH-4-d_2 was chosen as a deuteride donor and reacted with $\mathbf{nH^+}$ in methanolic solution (cf. Experimental Section). Reduction of $\mathbf{3H^+}$ proceeded rather sluggishly requiring 4 days at 20 °C for completion. Reduction of $\mathbf{4H^+}$ and $\mathbf{5H^+}$ proceeded more smoothly; a reaction time of 3 h at 50 °C was routinely adopted. Partial ^{1}H NMR spectra showing the C(4)H_2 region of **nHD** (**n** = **3**, **4**, **5**) as well as that of $\mathbf{nH_2}$ for comparison are collected in Figure 2. For **n** = **4** and **5** the C(4)HD signal is a single line at a chemical shift corresponding to H_A in $\mathbf{nH_2}$. As expected the presence of the geminal nucleus (D_B) leads to a significant broadening of the H_A signal as well as to a slight upfield shift (~0.03 ppm). Introduction of deuterium into $\mathbf{4H^+}$ and $\mathbf{5H^+}$ is thus found to proceed with a high degree of diastereoface-differentiation leading to the $\mathbf{nH_AD_B}$ diastereomer with a diastereomeric purity estimated to be ≥92%.

Interconversion between the diastereomers might in principle occur via rotation of Ar about the bonds connecting it to the bridge, a rotation that seems quite improbable from model considerations. Experimentally no isomerization could be detected even after prolonged (5 h at 60 °C) heating of $CDCl_3$ solutions of $\mathbf{4H_AD_B}$ and $\mathbf{5H_AD_B}$. The NMR spectrum of **3HD** (Figure 2) reveals that this product is formed with a much smaller degree of diastereoface-differentiation than **4HD** and **5HD**. A high-field singlet attributable to $\mathbf{3H_BD_A}$ and a weaker low-field singlet attributable to $\mathbf{3H_AD_B}$ indicate these diastereomers to be formed in a 2:1 ratio, which implies a diastereo-differentiation of only 67%. Furthermore the spectrum of **3HD** clearly indicates the presence of some of the undeuterated compound $\mathbf{3H_2}$. The hydride incorporated in the latter cannot originate from the reducing agent BNAH-4-d_2, which has an isotopic purity exceeding 98%. As indicated above, however, the reduction of $\mathbf{3H^+}$ proceeds much slower than that of either $\mathbf{4H^+}$ or $\mathbf{5H^+}$. Therefore **3HD** and $\mathbf{3H^+}$ coexist for a prolonged time in the reaction mixture, and it is assumed that hydride transfer between these species ($\mathbf{3HD + 3H^+ \rightarrow 3D^+ + 3H_2}$) is responsible for the formation of $\mathbf{3H_2}$.

(2.4) Diastereotopos-Differentiation[7] in the Reaction nHD → $\mathbf{nH^+}$ ($\mathbf{nD^+}$). As shown in the preceding section the diastereomers $\mathbf{4H_AD_B}$ and $\mathbf{5H_AD_B}$ could be prepared with a high degree of diastereomeric purity (≥92%). The diastereotopos-differentiation upon hydride (deuteride) abstraction from these compounds was investigated by using the 10-methylacridinium ion ($\mathbf{AcH^+}$) as a hydride acceptor. The ratio of hydride to deuteride transfer was readily determined by mass spectroscopic determination[22] (field-ionization technique, cf. Experimental Section) of the ratio of 10-methylacridan ($\mathbf{AcH_2}$) and monodeuterio-10-methylacridan (AcHD) produced in the reaction:

$$\mathbf{nH_AD_B + AcH^+ \rightarrow nH^+ (nD^+) + AcHD (AcH_2)}$$

The reaction was carried out in dimethyl sulfoxide at 20 °C and a twofold excess of $\mathbf{nH_AD_B}$ was used to avoid hydride exchange[23] between **AcHD** and unreacted $\mathbf{AcH^+}$.

From a similar reaction of the model compound **6HD** with $\mathbf{AcH^+}$ a primary isotope effect $I = k_H/k_D = 5.7$ was determined. This may be compared with $I = 4.5$ reported[22] for the reaction of $\mathbf{AcH^+}$ with the more reactive BNAH-4-d_1 in a variety of solvents. The ratio $P = \mathbf{AcHD/AcH_2}$ observed for reaction of both $\mathbf{4H_AD_B}$ and $\mathbf{5H_AD_B}$ with $\mathbf{AcH^+}$ was $P = 1.55 \pm 0.05$. Thus deuteride is abstracted preferentially notwithstanding the isotope effect which favors hydride abstraction. If it is assumed that the isotope effect ($I = 5.7$) determined for reaction of **6HD** with $\mathbf{AcH^+}$ also applies to reaction at both diastereotopic positions in **4HD** and **5HD** the reactivity ratio (S) of these positions can be calculated from

$$S = k_{H_B}/k_{H_A} = PI = 8.8$$

This corresponds to a diastereotopos-differentiation of 90%. It should be realized that this number represents a lower limit since complete diastereomeric purity of $\mathbf{nH_AD_B}$ has been assumed in its calculation. The presence of small amounts of the other diastereomer $\mathbf{nH_BD_A}$, which carries the most reactive isotope at the most reactive position, may markedly lower the ratio P observed. A worst case analysis assuming the presence of 8% of $\mathbf{nH_BD_A}$ indicates that in that case the degree of diastereoface-differentiation ought to be 93.5% ($S = 14.1$) to account for the experimental observations.

(2.5) Pseudoaxial vs. Pseudoequatorial Hydride Exchange. The data from the two preceding sections prove that a marked degree of diastereo-differentiation (≥90%) occurs during hydride exchange at cyclophanes **4** and **5** while a smaller, but still significant differentiation (~67%) occurs at **3**. Since X-ray diffraction and electronic absorption spectroscopy have provided evidence (vide

(15) Stam, C. H., unpublished results.
(16) Karle, I. L. *Acta Crystallogr.* **1961**, *14*, 497–502.
(17) Kuthan, J.; Musil, L. *Collect. Czech. Chem. Commun.* **1977**, *42*, 857–866.
(18) Kuthan, J.; Musil, L. *Collect. Czech. Chem. Commun.* **1975**, *40*, 3169–3176.
(19) van der Veen, R. H.; Kellogg, R. M.; Vos, A.; van Bergen, T. J. *J. Chem. Soc., Chem. Commun.* **1978**, 923–924.
(20) Triggle, A. M.; Shefter, E.; Triggle, D. J. *J. Med. Chem.* **1980**, *23*, 1442–1445.
(21) The labels A and B are assigned to the low- and high-field C(4) position, respectively. This assignment is identical[6] with that of the C(4) hydrogens in NADH, but of course no *pro-R*/*pro-S* stereochemical relationship is implied in the cyclophanes!
(22) van Laar, A.; van Ramesdonk, H. J.; Verhoeven, J. W. *Recl. Trav. Chim. Pays-Bas* **1983**, *102*, 157–163.
(23) Powell, M. F.; Bruice, T. C. *J. Am. Chem. Soc.* **1982**, *104*, 5834–5836.

supra) for a significant nonplanarity of the dihydropyridine chromophore in the cyclophanes $\mathbf{nH_2}$, it seems of interest to identify the orientation (i.e., pseudoequatorial or pseudoaxial) of the site at which hydride exchange preferentially occurs. For $\mathbf{3H_2}$ this is the magnetically least shielded site (i.e., site "A"), while it is the most shielded site ("B") for $\mathbf{4H_2}$ and $\mathbf{5H_2}$. Differential shielding of H_A and H_B may arise from a different orientation with respect to the magnetically anisotropic Ar group as well as from an intrinsic anisochronism induced by the distortion of the dihydropyridine ring.

The UV and X-ray data indicate that the latter effect is equally small in all cyclophanes containing a 1,4-connected Ar group ($\mathbf{1H_2}$–$\mathbf{3H_2}$). Therefore the large anisochronism of H_A and H_B in $\mathbf{3H_2}$ must be attributed to the "ring-current" effect of the naphthalene group. The crystal structure of $\mathbf{1H_2}$ (cf. Figure 1) provides some insight in the orientation of the C(4) hydrogens with respect to a 1,4-connected Ar group. The pseudoequatorial hydrogen (H_{42} in Figure 1) impinges upon the center of the Ar group (i.e., upon the center of the substituted ring of the naphthalene system in $\mathbf{3H_2}$) and lies only 2.72 Å above the Ar plane. The pseudoaxial hydrogen (H_{41} in Figure 1) has a much larger distance (3.71 Å) to this plane.

Application of the Johnson and Bovey[24] shielding model—treating the magnetic effect of a naphthalene system as that of two independent benzene rings—leads to a predicted shielding of the equatorial C(4) proton in $\mathbf{3H_2}$ which exceeds that of the axial C(4) proton by ~1 ppm. This compares reasonably well with the experimental value (cf. Table I) $\delta_{H_A} - \delta_{H_B} = 0.69$ ppm and thus leaves no doubt that in $\mathbf{3H_2}$ the pseudoaxial and pseudoequatorial positions can be assigned to H_A and H_B, respectively.

For the cyclophanes $\mathbf{4H_2}$ and $\mathbf{5H_2}$ the assignment of the orientation of H_A and H_B on the basis of their relative chemical shifts seems rather arbitrary. The 1,3-connectivity of the Ar group in these cyclophanes leads to a conformation in which the projection of C(4) is shifted from the center of Ar to a position at or beyond its edge. As a result the shielding effect of Ar on both C(4) hydrogens is diminished as compared to that in $\mathbf{1H_2}$ or $\mathbf{2H_2}$ (cf. Table I). Interpretation of the origin of the small chemical shift difference ($\delta_{H_A} - \delta_{H_B} \approx 0.1$ ppm) observed in $\mathbf{4H_2}$ and $\mathbf{5H_2}$ is complicated further by the strong distortion of the dihydropyridine ring in these cyclophanes. Such distortion may induce a chemical shift difference between axial and equatorial positions opposite[3] to that induced by the "external" anisotropy effect of the Ar group.

As evident from model studies as well as from the X-ray structure of $\mathbf{1H_2}$ (Figure 1) the amide NH protons and the $C(4)H_2$ protons form a tightly packed cluster in the compounds $\mathbf{nH_2}$. For a planar geometry the distances that separate both C(4) hydrogens from the NH hydrogens are equal but distortion to a pseudoboat geometry shortens that distance for the pseudoequatorial C(4)H while that for the pseudoaxial C(4)H is lengthened. Thus difference nuclear Overhause effect (NOE) spectra[25] of $\mathbf{4H_2}$ and $\mathbf{5H_2}$ were measured in which the amide NH protons are saturated. As expected, rather strong positive NOE effects were observed for both $C(4)H_A$ and $C(4)H_B$, the effect being about twice as strong for the former. This unequivocally identifies the low-field ($C(4)H_A$) position as pseudoequatorial and the high-field ($C(4)H_B$) position as pseudoaxial in both $\mathbf{4H_2}$ and $\mathbf{5H_2}$, which corroborates our earlier[1] tentative assignment for $\mathbf{4H_2}$.

As hydride exchange occurs preferentially at the least shielded position (H_A) in $\mathbf{3H_2}$ and at the most shielded position (H_B) in $\mathbf{4H_2}$ and $\mathbf{5H_2}$ this may now be concluded to be the pseudoaxial position in all cases. Interestingly enhanced reactivity of the axial over the equatorial position has been postulated as early as 1957 by Levy and Vennesland.[8] Recently the possible stereoelectronic nature of such an enhancement resulting from the parallel alignment of the axial C(4)–H bond and the (dihydro)pyridine π-orbitals has been stressed.[10,26] The relevance of such stereoelectronic effects to the explanation of the diastereo-differentiating hydride exchange at our cyclophanes as well as at NAD(H) under enzymatic conditions will be discussed in the following sections in the light of the results of kinetic measurements on both hydride addition and abstraction.

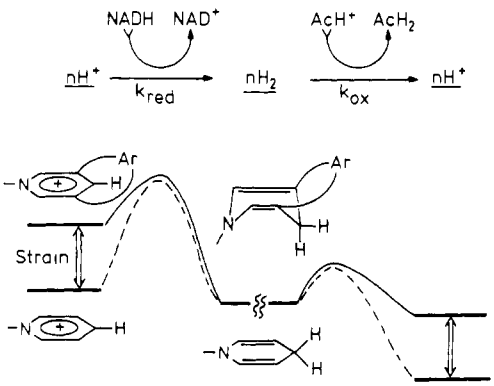

Figure 3. Schematic energy profiles for redox processes of the pyridinium/dihydropyridine system in the absence (broken line) and in the presence (solid line) of a bridging group which leads to distortion at the dihydropyridine stage. Energies have been normalized at the dihydropyridine stage.

Table III. Kinetic Data for the Interconversion of Bridged ($\mathbf{n = 1–5}$) and Nonbridged ($\mathbf{n = 6}$) Coenzyme Models between Their Oxidized ($\mathbf{nH^+}$) and Reduced ($\mathbf{nH_2}$) Form via Reduction with NADH and Oxidation with AcH^+ Respectively

$$\mathbf{nH^+} + \mathrm{NADH} \xrightarrow{k_{red}} \mathbf{nH_2} + \mathrm{NAD^+}$$

$$\mathbf{nH_2} + \mathrm{AcH^+} \xrightarrow{k_{ox}} \mathbf{nH^+} + \mathrm{AcH_2}$$

n	$10^4 k_{red}$, L mol^{-1} s^{-1} [a]	k_{ox}, L mol^{-1} s^{-1} [b]
1	34 ± 10%	0.9 ± 10%
2	71	1.1
3	120	0.7
4	9100	1.0
5	8700	1.4
6	1000	3.4

[a] In aqueous solution (pH 7) at 20 °C. [b] In acetonitrile at 20 °C.

(2.6) Kinetic Aspects of Hydride Exchange at the Cyclophanes. A comparison of the reactivity of (co)enzyme models with that of real enzymes is often thwarted by the irreversible nature of the model reactions studied.[27,28] This prohibits[29] discrimination between purely catalytic effects (i.e., effects limited to the transition state) and effects that influence substrate and product stability as well.

The individual hydride-addition and -abstraction reactions described above clearly are also irreversible from any practical point of view. Nevertheless they are strongly related mechanistically[22] and together they provide a quasi-reversible interconversion of the cyclophanes between their oxidized ($\mathbf{nH^+}$) and reduced forms ($\mathbf{nH_2}$). The combined kinetic data of these processes may thus yield valuable information regarding the factors that govern the rate and the diastereo-differentiation of this interconversion.

Such kinetic information was now gathered for the reduction (k_{red}) of $\mathbf{nH^+}$ with β-NADH in aqueous solution, as monitored spectrophotometrically, and for oxidation (k_{ox}) of $\mathbf{nH_2}$ by AcH^+ in acetonitrile, as monitored by fluorescence spectroscopy (cf. Table III).

(24) Bovey, F. E. "Nuclear Magnetic Resonance Spectroscopy"; Academic Press: New York, 1969.
(25) Anet, F. A. L.; Bourn, A. J. R. *J. Am. Chem. Soc.* **1965**, *87*, 5250–5251.
(26) Buck, H. M., personal communication.
(27) Graafland, T.; Wagenaar, A.; Kirby, A. J.; Engberts, J. B. F. N. *J. Am. Chem. Soc.* **1979**, *101*, 6981–6991.
(28) Cram, D. J.; Edan Katz, H. *J. Am. Chem. Soc.* **1983**, *105*, 135–137.
(29) An interesting and vivid discussion of this problem is given by: Breslow, R.; Cram, D. J. *Chem. Eng. News* **1983**, *61*, 4 and 59.
(30) These signs correspond to those found by MINDO-3 calculations for the HOMO of the 1,4-dihydropyridine system (van der Kerk, S. M.; van Gerresheim, W., Verhoeven, J. W., unpublished results).

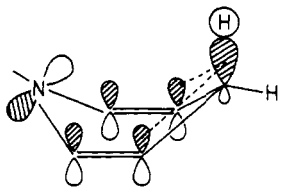

Figure 4. Bonding π-type overlap between the HOMO of the π-system and the LUMO of the partial C–H bond in an axial transition state for hydride transfer at a distorted pyridine ring. The relative sign[30] of the orbital lobes is indicated by shading, their size has been chosen arbitrarily.

The reduction of the cyclophanes containing a 1,3-connected Ar group in the bridge (i.e., $\mathbf{4H^+}$ and $\mathbf{5H^+}$) proceeds 100–300 times faster than that of the less strained cyclophanes containing a 1,4-connected Ar group ($\mathbf{1H^+}$–$\mathbf{3H^+}$). This rate enhancement thus seems to be related to a significant relief of strain in the transition state for reduction of $\mathbf{4H^+}$ and $\mathbf{5H^+}$. As we have noted above relief of strain in the reduced form (i.e. $\mathbf{4H_2}$ and $\mathbf{5H_2}$) is achieved by distortion of the flexible dihydropyridine chromophore and apparently this distortion already makes itself felt in the transition state of the reduction process.

Further information regarding the degree of distortion in the transition state may be gained from inspection of the k_{ox} values compiled in Table III. These show that for all cyclophanes the energy gap separating $\mathbf{nH_2}$ and the transition state is nearly identical. It is thus concluded that the relief of strain resulting from dihydropyridine distortion in $\mathbf{nH_2}$ is fully retained in the transition state and therefore has no influence on k_{ox} but a large influence on k_{red}. This situation is schematized in Figure 3 where the solid line and the broken line delineate the energy of a strained system (like $\mathbf{4H^+/4H_2}$ and $\mathbf{5H^+/5H_2}$) and a hypothetical unstrained system along the reaction coordinate of their reduction and oxidation processes. The energies have been normalized at the reduced stage.

For comparison the k_{ox} and k_{red} values measured for a nonbridged system ($\mathbf{6H^+/6H_2}$) have also been compiled in Table III. The k_{red} value is found to be intermediate between that of the "slow" and the "fast" cyclophanes, while the k_{ox} value is about 3 times higher than that of the cyclophanes. The latter effect seems mainly related to the steric hindrance that the bridge imposes upon approach of the oxidizing reagent toward the cyclophanes. For this effect a factor of 2 might be predicted if the bridge were assumed to shield one face of the pyridine ring specifically.

From the discussion above it must be concluded that pyridine ring distortion not only occurs at the reduced stage ($\mathbf{nH_2}$) of strained cyclophanes but also at the transition state for conversion between $\mathbf{nH^+}$ and $\mathbf{nH_2}$. This implies that the C(4)–H bond made or broken during this conversion can either adopt a pseudoaxial or a pseudoequatorial orientation in the transition state. Simple stereoelectronic considerations[10,17] suggest the axial transition state to be stabilized by π-type overlap (hyperconjugation) between the partial C–H bond and the ring π-system (see Figure 4). Thus stereoelectronic effects may be largely responsible for the high degree of diastereo-differentiation in hydride transfer at the most strained cyclophanes ($\mathbf{n} = 4$ and 5), in addition to the effect of differential reagent accessibility at the two faces of the pyridine ring.

(2.7) Diastereo-Differentiation in Enzymatic Systems. Various types of enzyme-induced conformational changes in enzyme-bound pyridine dinucleotide coenzymes have been suggested to play a role in determining the diastereo-differentiating course of enzyme-catalyzed hydride transfer. As early as 1957 Levy and Vennesland proposed[8] that the dihydropyridine ring of the reduced coenzyme adopts a pseudoboat conformation in the holo-enzyme, which places the C(4) hydrogens at psdeudoaxial and pseudoequatorial positions.[31,32] As discussed above (cf. Figure 4) stereoelectronic considerations[10,17] suggest the pseudoaxial C–H bond to be most reactive.

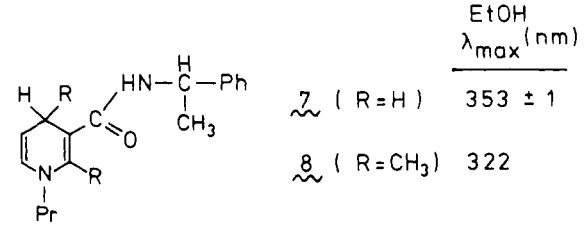

Figure 5. Structure and UV absorption maxima for **7** and **8** (adapted from ref 33).

Another type of conformational change that might lead to differential reactivity of the diastereotopic C(4) positions was recently proposed by Buck et al.[9] This involves rotation of the plane of the C(3) amide group with respect to the plane of the pyridine ring, the enzyme dictating the sense of rotation and thereby the type of diastereo-differentiation (A or B).

The results of our present study on bridged NAD(H) models allow an unprecedented insight into the feasibility of these proposals. At first sight the large degree of diastereo-differentiation observed for hydride transfer at the strained cyclophanes ($\mathbf{n} = 4$ and 5) seems to support the model put forward by Levy and Vennesland.[8,31,32] Our results, however, also indicate that a distortion of the dihydropyridine ring sufficiently large to induce significant diastereo-differentiation leads to a large blue shift of the dihydropyridine electronic absorption (cf. Table II).

Interestingly the same applies to the effect of rotation of the amide group with respect to the dihydropyridine ring of a 1,4-dihydronicotinamide. This can be concluded from the reported[33] absorption data of **7** and **8** (see Figure 5). In **7** the amide group is free to adopt a position of maximum conjugation with the dihydropyridine ring but in **8** the methyl substituents at C(2) and C(4) enforce a twist angle of 65° about the C(3)–amide bond.[34]

The effect of complexation between various dehydrogenases and NAD(P)H on the electronic absorption of the coenzyme has been investigated by difference spectroscopy.[35] Depending on the enzyme used both red and blue shifts were reported to occur, the former being more pronounced! Thus a red shift of 11 ± 2 nm was determined[35] for NADH upon complexation with glyceraldehyde-phosphate dehydrogenase (GDPH). The reliability of the difference spectroscopy technique may be questioned, however, especially because correction ought to be made[36] for partial hydratation of NAD(P)H catalyzed by the enzyme, which otherwise leads to a large apparent hypochromicity. For the NADH/GDPH complex a more reliable determination of the NADH absorption maximum was recently achieved by CD spectroscopy.[37] The value obtained (335 nm) implies a minor blue shift with respect to the free coenzyme (340 nm). These small shifts may readily be accounted for by the effect of transfer from water to a less polar environment at the active site of the enzyme. Table II shows an analogous blue shift for $\mathbf{6H_2}$ upon transfer from water to Me_2SO.

It is thus concluded that in the active site of dehydrogenase the dihydronicotinamide chromophore of NAD(P)H undergoes no extensive distortions comparable to those found in $\mathbf{4H_2}$, $\mathbf{5H_2}$, or **8**. Of course a transient distortion[9] during the transition state of the enzymatic process cannot be ruled out. However, substitution of the C(3) amido group in NAD^+ by a C(3) cyano group was found[38] to have no influence on the stereochemical course of the reduction under enzymatic conditions. This seems to rule out

(31) Velick, S. F. *J. Biol. Chem.* **1958**, *233*, 1455–1467.
(32) Wallenfels, K.; Hofman, D. *Tetrahedron Lett.* **1959**, *15*, 10–13.
(33) Ohno, A.; Ikeguchi, M.; Kimura, T.; Oka, S. *J. Am. Chem. Soc.* **1979**, *101*, 7036–7040.
(34) van Lier, P. M.; Donkersloot, M. C. A.; Koster, A. S.; van Hoff, H. J. G.; Buck, H. M. *Recl. Trav. Chim. Pays-Bas* **1982**, *101*, 119–120.
(35) Fisher, H. F.; Adija, D. L.; Cross, D. G. *Biochemistry* **1969**, *8*, 4424–4431.
(36) Hilvers, A. G.; Weenen, J. H. M.; van Dam, K. *Biochem. Biophys. Acta* **1966**, *128*, 74–81.
(37) Boers, W.; Oosthuizen, C.; Slater, E. C. *Biochim. Biophys. Acta* **1971**, *250*, 35–46.
(38) Biellmann, J. F.; Hirth, C. G.; Jung, M. J.; Rosenheimer, N.; Wrixon, A. D. *Eur. J. Biochem.* **1974**, *41*, 517–524.

an enzyme-dictated rotation of the amide group as a factor of major importance in determining enzymatic diastereo-differentiation.

Our results thus clearly indicate that dehydrogenases must use mechanisms other than distorting the dihydronicotinamide chromophore to produce their virtually complete diastereo-differentiation. It seems attractive to suggest that this is linked to the huge catalytic activity of enzymes. Since the degree of diastereo-differentiation is determined by the *ratio* of the rate constants for transfer of H_A and H_B, a high degree of differentiation can not only be achieved by selective inhibition at one site (i.e. by "negative-differentiation") but also by selective catalysis (i.e., by "positive-differentiation"). An interesting model that leads to such positive-differentiation was recently proposed by Benner et al.,[11,12] who pointed out that specific catalysis at H_A or H_B may result if the enzyme binds its cofactor with the nicotinamide ring oriented anti or syn, respectively, relative to the ribose unit. Furthermore the fascinating proposal was made that this orientation not only determines the stereochemistry of hydride transfer but also influences the reducing power of the coenzyme, thus finely tuning this to the demands of the particular substrate and thereby optimizing the catalytic efficiency of the enzymatic system.

3. Experimental Section

(3.1) Instrumentation. UV and fluorescence measurements were performed with a Cary-17D and a Spex-Fluorolog spectrometer. Mass spectra were recorded on a Varian MAT 711 double-focusing mass spectrometer. For accurate determination of deuterium contents the field-ionization technique was applied as described extensively before.[22] ^{1}H NMR spectra were recorded on Bruker 250- and 360-MHz Fourier-transform spectrometers.

(3.2) Reagents. The reagents **BNAH**, **BNAH-4-d_2**, and **AcH$^+$** were obtained as described earlier.[22] Synthesis of **6H$_2$** has also been described before.[39]

(3.3) Synthesis of Cyclophanes nH (n = 1–5). All cyclophanes **nH** (**n = 1–5**) were obtained by condensation[40] of pyridine-3,5-dicarbonyl dichloride (**9**) with the appropriate diamine $H_2NCH_2CH_2ArCH_2CH_2NH_2$ under high dilution.[40] These diamines were prepared by standard routines extensively described elsewhere.[41]

Pyridine-3,5-dicarbonyl Dichloride (9). Pyridine-3,5-dicarboxylic acid monohydrate (50 g, 0.27 mol) was refluxed with thionyl chloride (250 mL) until a clear solution formed. The excess thionyl chloride was removed in vacuo and the residue was recrystallized twice from *n*-hexane under an atmosphere of dry nitrogen. Infrared analysis indicated complete conversion of the carboxylate groups. Yield, 45 g (~85%); IR (KBr) 3000 (ν_{CH}), 1740 ($\nu_{C=O}$) cm^{-1}.

Cyclophane 1H. Separate solutions were prepared of **9** (2 g, 10 mmol) and 1,4-bis(2-amino-1-ethyl)benzene (1.6 g, 10 mmol) in dry toluene (500 mL each). These solutions were slowly added at room temperature under an atmosphere of dry nitrogen to a well-stirred reaction vessel containing a solution of triethylamine (2 g, 20 mmol) in 2 L of dry toluene. The addition was accomplished by means of a two-channel peristaltic metering pump over a period of 50 h. Polymeric material and triethylamine hydrochloride were removed by filtration. After removal of the solvent in vacuo the residue was chromatographed over silica with ethanol/ethyl acetate (1:20) as an eluent. The cyclophane (identified by MS) elutes before higher oligomers. Final purification was achieved by recrystallization from ethanol. Yield, 0.1 g (3%); MS, *m/z* 295 ($C_{17}H_{17}N_3O_2$); IR (KBr) 3300 (ν_{NH}), 1630 ($\nu_{C=O}$) cm^{-1}; ^{1}H NMR ($CDCl_3/CD_3OD$ 10:1)[42] δ 3.1 (CH_2Ar), 3.7 (CH_2N), 5.8 (C(4)H), 7.2 (Ar H), 8.8 (C(2)H, C(6)H).

Cyclophane 2H. This was prepared as described for **1H** by condensation of **9** (10 mmol) and 1,4-bis(2-amino-1-ethyl)-2,5-dimethoxybenzene (10 mmol). The structure of this cyclophane was confirmed by X-ray structure determination.[14] Yield, 0.25 g (7%); MS, *m/z* 355 ($C_{19}H_{21}N_3O_4$); IR (KBr) 3300 (ν_{NH}), 1640 ($\nu_{C=O}$) cm^{-1}; ^{1}H NMR ($CDCl_3/CD_3OD$ 10:1)[42] δ 2.8 (CH_2Ar), 3.7 (CH_2N), 3.7 (OCH_3), 5.9 (C(4)H), 6.7 (Ar H), 8.8 (C(2)H, C(6)H).

Cyclophane 3H. This was prepared as described for **1H** by condensation of **9** (17 mmol) and 1,4-bis(2-amino-1-ethyl)naphthalene (17 mmol). Yield, 0.15 g (2.5%); MS, *m/z* 345 ($C_{21}H_{19}N_3O_2$); IR (KBr) 3300 (ν_{NH}), 1650 ($\nu_{C=O}$) cm^{-1}; ^{1}H NMR ($CDCl_3/CD_3OD$ 10:1) δ 1.8 (NH), 3.3–4.4 (CH_2CH_2), 5.6 (C(4)H), 7.2–8.1 (Ar H), 8.8 (C(2)H, C(6)H).

Cyclophane 4H. This was prepared as described for **1H** by condensation of **9** and 1,3-bis(2-amino-1-ethyl)-2,4,6-trimethylbenzene. The preparation was repeated several times with yields varying between 2% and 10% (after recrystallization from ethanol). MS, *m/z* 337 ($C_{20}H_{23}N_3O_2$); IR (KBr) 3320 (ν_{NH}), 1640 ($\nu_{C=O}$) cm^{-1}; ^{1}H NMR ($CDCl_3$)[42] δ 2.1 ($ArCH_3$), 2.4 ($ArCH_3$ (2x)), 2.6–4.3 (CH_2CH_2), 6.7 (C(4)H), 6.9 (Ar H), 8.8 (C(2)H, C(6)H).

Cyclophane 5H. This was prepared as described for **1H** by condensation of **9** and 2,4-bis(2-amino-1-ethyl)-3,5-dimethylanisole, in a yield of about 3% (recrystallization from ethanol/water). The structure of this cyclophane was confirmed by X-ray structure analysis.[15] Accurate MS, *m/z* 353.17364 (calcd 353.17393 for $C_{20}H_{23}N_3O_3$); IR ($CHCl_3$) 3460, 3400 (ν_{NH}), 1660 ($\nu_{C=O}$) cm^{-1}. ^{1}H NMR ($CDCl_3$)[42] δ 2.0 ($ArCH_3$), 2.38 ($ArCH_3$), 2.6–4.3 (CH_2CH_2), 3.8 (OCH_3), 6.63 (C(4)H and Ar H) and 8.8 (C(2)H, C(6)H).

(3.4) Synthesis of Cyclophanes nH$^+$ (n = 1–5). Cyclophanes **nH$^+$** were obtained by quaternization of **nH** with benzyl bromide.

Cyclophane 1H$^+$. A mixture of **1H** (170 mg, 0.58 mmol) and benzyl bromide (2 mL) was heated at 80 °C during 1 h. After cooling the reaction mixture was diluted with methanol (ca. 0.5 mL) and then poured into 100 mL of dry ether. The precipitate was isolated by filtration and purified by recrystallization from ethanol. Yield, 180 mg (67%); IR (KBr) 3400, 3200 (ν_{NH}), 1650 ($\nu_{C=O}$) cm^{-1}; ^{1}H NMR (CD_3OD)[42] δ 3.0 (CH_2Ar), 3.7 (CH_2NCO), 5.9 (CH_2Ph), 6.1 (C(4)H), 7.2 (Ar H), 7.5 (PhH), 9.2 (C(2)H, C(6)H).

Cyclophane 2H$^+$ was obtained from **2H** and benzyl bromide as described for **1H$^+$** in a yield of 81%. IR (KBr) 3400, 3220 (ν_{NH}), 1670 ($\nu_{C=O}$) cm^{-1}; ^{1}H NMR (CD_3OD)[42] δ 2.8 (CH_2Ar), 3.7 (OCH_3), 4.0 (CH_2NCO), 5.9 (CH_2Ph), 6.6 (C(4)H), 6.8 (Ar H), 7.5 (PhH), 9.3 (C(2)H, C(6)H).

Cyclophane 3H$^+$ was obtained from **3H** and benzyl bromide as described for **1H$^+$** in 90% yield. IR (KBr) 3500 (ν_{NH}), 1655 ($\nu_{C=O}$) cm^{-1}. ^{1}H NMR (CD_3OD) 3.3–4.3 (CH_2CH_2), 5.8 (CH_2Ph), 6.3 (C(4)H), 7.2–8.1 (Ar H, PhH), 9.2 (C(2)H, C(6)H).

Cyclophane 4H$^+$ was obtained from **4H** and benzyl bromide as described for **1H$^+$** in 70% yield (recrystallization from ethanol/diethyl ether); IR (KBr) 3400, 3220 (ν_{NH}, 1655 ($\nu_{C=O}$) cm^{-1}; ^{1}H NMR (CD_3OD)[42] δ 1.58 and 2.07 (CH_3 at C(2) of Ar), 2.34 and 2.39 (CH_3 (2x) at C(4) and C(6) of Ar), 2.7–3.6 (CH_2CH_2), 5.92 (CH_2Ph), 6.14 and 7.13 (C(4)H), 6.99 (Ar H), 7.5 (PhH), 9.24 and 9.27 (C(2)H, C(6)H).

Cyclophane 5H$^+$ was obtained from **5H** and benzyl bromide as described for **1H$^+$** in 80% yield (recrystallization from ethanol/diethyl ether). IR ($CHCl_3$) 3400 (ν_{NH}), 1675 ($\nu_{C=O}$) cm^{-1}; ^{1}H NMR (CD_3OD)[42] δ 1.68 and 2.20 (CH_3 at C(3) of Ar), 2.58 and 2.63 (CH_3 at C(5) of Ar), 2.5–4.0 (CH_2CH_2), 4.03 (OCH_3), 6.00 and 6.06 (CH_2Ph), 6.58 and 7.29 (C(4)H), 6.98 (Ar H), 7.6–7.8 (PhH), 9.41 and 9.46 (C(2)H, C(6)H).

(3.5) Synthesis of Cyclophanes nH$_2$ (n = 1–5). Cyclophanes **nH$_2$** were obtained from **nH$^+$** by reduction with an equimolar amount of BNAH.

Cyclophane 1H$_2$. A solution of **1H$^+$** (145 mg, 0.31 mmol) and BNAH (66 mg, 0.31 mmol) in methanol (5 mL) was stirred at 50 °C for 3 h under a nitrogen atmosphere in the dark. Water was added to the cooled reaction mixture to precipitate **1H$_2$**. This was isolated by filtration and purified by recrystallization from ethanol/water (1:1), yield 64 mg (53%), yellow solid. The structure of this cyclophane was confirmed by X-ray structure analysis.[14] ^{1}H NMR ($CDCl_3$) δ 1.95 (C(4)H$_2$), 3.00 (CH_2Ar), 3.62 (CH_2NCO), 4.44 (CH_2Ph), 4.66 (NH), 7.01 (C(2)H, C(6)H), 7.15 (Ar H), 7.24 (PhH).

Cyclophane 2H$_2$ was prepared from **2H$^+$** and BNAH as described for **1H$_2$** in 59% yield. ^{1}H NMR ($CDCl_3$) δ 2.08 (C(4)H$_2$), 2.6 (CH_2Ar), 3.4 (CH_2NCO), 3.64 (OCH_3), 4.42 (CH_2Ph), 5.0 (NH), 6.59 (Ar H), 6.99 (C(2)H, C(6)H), 7.26 (PhH).

Cyclophane 3H$_2$ was prepared from **3H$^+$** and BNAH as described for **1H$_2$** in 54% yield. MS, *m/z* 437 ($C_{28}N_{27}N_3O_2$); ^{1}H NMR ($CDCl_3$) δ 1.43 (C(4)H$_B$), 2.12 (C(4)H$_A$), 3.29–3.42 (CH_2Ar), 3.59–4.18 (CH_2NCO), 4.50 (CH_2Ph), 4.53 (NH), 7.07 (C(2)H, C(6)H), 7.1–8.1 (Ar H, PhH).

Cyclophane 4H$_2$ was prepared from **4H$^+$** and BNAH as described for **1H$_2$** in 71% yield. Accurate MS, *m/z* 429.2419 (calcd 429.2416 for $C_{27}H_{31}N_3O_2$); ^{1}H NMR ($CDCl_3$) δ 1.99 ($ArCH_3$), 2.33 ($ArCH_3$ (2x)), 2.48 (C(4)H$_B$), 2.61 (C(4)H$_A$), 2.8–4.3 (CH_2CH_2), 4.64 (CH_2Ph), 5.48 (NH), 6.9 (Ar H), 7.30 (C(2)H, C(6)H), 7.35 (PhH).

(39) Hays, G. R.; Huis, R.; Coleman, B.; Clague, D.; Verhoeven, J. W.; Rob, F. *J. Am. Chem. Soc.* **1981**, *103*, 5140–5146.

(40) Dittmer, D. C.; Blidner, B. B. *J. Org. Chem.* **1973**, *38*, 2873–2882.

(41) Rob, F. PhD Dissertation, University of Amsterdam, The Netherlands, 1983.

(42) NMR signals of cyclophanes **nH** and **nH$^+$** (**n = 1, 2, 4,** and **5**) show broadening or splitting at room temperature due to the presence of interconverting conformers. Variable-temperature NMR studies are described elsewhere.[41,43]

(43) Rob, F.; Verhoeven, J. W., unpublished results.

Cyclophane $5H_2$ was prepared from $5H^+$ and BNAH as described for $1H_2$ in 78% yield. ^1H NMR $CDCl_3$) δ 1.95 ($ArCH_3$), 2.36 ($ArCH_3$), 2.48 ($C(4)H_B$), 2.56 ($C(4)H_A$), 2.8-4.2 (CH_2CH_2), 3.82 (OCH_3), 4.60 (CH_2Ph), 5.41 (NH), 6.62 (Ar H), 7.30 (C(2)H, C(6)H), 7.35 (PhH).

(3.6) Deuterium Incorporation. The monodeuterated compounds **nHD** (**n** = 3-6) were prepared by reaction of the appropriate pyridinium ion (nH^+) with an equimolar amount of BNAH-4-d_2. For n = 4-6 the same reaction conditions were applied as described above for the conversion $1H^+ \rightarrow 1H_2$. Under these conditions formation of **3HD** gave no satisfactory results. In this case the reaction was performed at 20 °C during 4 days (yield 64%).

(3.7) Oxidation of nHD by AcH^+. Compounds **4HD**, **5HD**, and **6HD** were subjected to oxidation by AcH^+ and the deuterium content of the 10-methylacridan thus obtained was determined by MS (field-ionization technique). To avoid isotopic exchange[23] between acridan and unreacted AcH^+ the reactions were carried out with a twofold excess of **nHD**. Typically solutions of **nHD** (0.6 mmol) and AcH^+ (0.3 mmol) in dimethyl sulfoxide (2 mL each) were mixed and stirred for 1 h at 20 °C. The reaction mixture was than poured in ice water and the white precipitate of 10-methylacridan collected by filtration and purified by recrystallization from ethanol/water 2:1.

Determination of the deuterium content was performed by MS using the field-ionization (FI) technique as described extensively before.[22] MS-FI was found[22] to avoid the problem of erratic M/M + 1 ratios, which thwarts MS measurements on 10-methylacridan under electron-impact conditions. All MS-FI measurements were repeated at least 5 times. The following peak ratios m/z 195/196/197 were observed in the molecular ion region: 55.4/100/22.1 for the product from reaction of AcH^+ with **4HD** and 56.1/100/23 from the reaction with **5HD**. The reference experiment with **6HD** gave a ratio 100/38.5/4.5 while unlabeled AcH_2 gave 100/21.1/zero.

(3.8) Kinetic Procedures. The rate of reduction of nH^+ was studied with β-NADH (Merck) as a reductant in aqueous solution at 20 °C. In all cases the reduction product nH_2 absorbs at longer wavelength (see Table II) than **NADH** (λ_{max} = 340 nm, ϵ = 6220 L mol^{-1} cm^{-1}), which allowed the reaction to be followed by monitoring the increase of absorption at a wavelength (λ > 400 nm) where the absorption of NADH may be neglected.

For the reactive systems (**n** = **4**, **5**, **6**) the reactions were carried out under second-order conditions with equal initial concentrations of NADH and nH^+ (both $\sim 10^{-4}$ mol L^{-1}). For the less reactive systems the reaction is unduly slow at these concentrations and the spontaneous decomposition of NADH (mainly by hydratation) becomes competitive. Therefore a tenfold excess of nH^+ ($\sim 10^{-3}$ mol L^{-1}) was employed for **n** = **1**, **2**, and **3**. In all cases isosbestic points were observed over at least two **NADH** half-lifetimes and linear second order (**n** = **4**, **5**, **6**) and pseudofirst-order (**n** = **1**, **2**, **3**) kinetic plots were obtained. Results are compiled in Table III. The rate of oxidation of nH_2 was studied with AcH^+ as an oxidant in acetonitrile at 20 °C. All reactions were measured under pseudo-first-order conditions with initial concentrations $nH_2 \approx 10^{-3}$ mol L^{-1} and $AcH^+ \approx 10^{-5}$ mol L^{-1}. The decrease of the AcH^+ concentration is very conveniently monitored by fluorescence spectroscopy. Selective excitation of AcH^+ was achieved at 450 nm. The strong green fluorescence (quantum yield near unity) occurs at 500 nm. Results are compiled in Table III.

Acknowledgment. We thank C. H. Stam (University of Amsterdam, Laboratory for Crystallography) for performance and discussion of the X-ray structure determinations. Measurement of the 360-MHz ^1H NMR spectra by R. Kaptein and K. Dijkstra (University of Groningen) is gratefully acknowledged. We thank C. Kruk et al. for extensive 250-MHz ^1H NMR and NOE measurements. FI-MS measurements were realized by the courtesy of N. M. M. Nibbering, R. H. Fokkens, and J. J. Zwinselman. We thank U. K. Pandit for stimulating discussions on the reactivity of NAD(H) models. The 360-MHz ^1H NMR facilities were made available- and part of these investigations was supported by the Netherlands Foundation for Chemical Research (SON) with financial aid from the Netherlands Organization for the Advancement of Pure Research (ZWO).

Resonant Fluorescence Study of the Eu^{3+}-Substituted Ca^{2+} Site in Busycon Hemocyanin: Structural Coupling between the Heterotropic Allosteric Effector and the Coupled Binuclear Copper Active Site

Yeong Tsyr Hwang,[†] Leonard J. Andrews,*[‡] and Edward I. Solomon*[†]

Contribution from the Department of Chemistry, Stanford University, Stanford, California 94305, and GTE Laboratories, Waltham, Massachusetts 02254.
Received September 12, 1983

Abstract: Eu^{3+} was substituted for Ca^{2+} as an allosteric effector in hemocyanin, and its laser-induced f-f fluorescence was studied to probe the allosteric effects on the Ca^{2+} binding site induced by deoxygenation of the binuclear copper active site. The $^7F_0 \rightarrow {}^5D_0$ excitation spectrum of Eu^{3+} was monitored to define two kinds of high-affinity Eu^{3+} binding sites in the hemocyanin biopolymer, one of which is competitive with the Ca^{2+} ion. The fluorescence decay lifetimes of this Ca^{2+}-competitive Eu^{3+} site were measured in D_2O and H_2O buffer which permitted an estimate of the coordinated water number at the Eu^{3+} ion. The results show that in the relaxed quaternary structure the Ca^{2+} site is located in a very hydrophilic environment with $\sim$5 H_2O molecules and $\sim$3 protein ligands in its first coordination sphere. When the coupled binuclear copper active site is deoxygenated, the Ca^{2+} site appears to release one coordinated water molecule upon binding an additional protein ligand. This may correlate to the allosteric role of Ca^{2+} in stabilizing the tense quaternary structure. Further, the internal energy transfer from the Eu^{3+} allosteric site to the coupled binuclear copper active site was monitored (using the met active site derivative) and used to estimate the average distance between these two sites to be $\sim$32 Å.

Under physiological conditions, mollusc hemocyanins are present as highly aggregated biopolymers with a molecular architecture composed of 20 subunits. Each subunit contains eight binuclear copper active sites covalently linked in a single polypeptide chain of about 400 000 daltons. Hemocyanin functions as an oxygen-carrying protein with a Cu:dioxygen ratio of 2:1. Oxygen binds as peroxide bridging two cupric ions, producing intense blue color with strong absorption in the regions of 345 and 570 nm,[1] corresponding to peroxide-to-copper(II) charge-

[†] Stanford University.
[‡] GTE Laboratories.

0002-7863/84/1506-3832$01.50/0